

# GEOMETRY, PENETRATION FORCE, AND CUTTING PROFILE OF DIFFERENT 23-GAUGE TROCARS SYSTEMS FOR PARS PLANA VITRECTOMY

CARSTEN H. MEYER, MD,\* HAKAN KAYMAK, MD,† ZENGPING LIU, MD,§ SANDEEP SAXENA, MD,\*  
EDUARDO B. RODRIGUES, MD‡

---

**Background:** To investigate the geometry, penetration force, and cutting profile of 23-gauge trocar systems for pars plana vitrectomy based on their grinding methods in a standardized laboratory setting.

**Methods:** In this experimental study, Eleven different commercially available 23-gauge sclerotomy trocar systems were divided into 4 groups according to their needle grinding and deburring: “back” bevel, “spear” bevel, “lancet” bevel, and “spatula” bevel. The normative geometrical data of the trocar systems were systematically analyzed according to nomenclature ISO 7864 and ISO 9626. Force to penetrate a 0.4-mm thick polyurethane foil was measured by a Penetrometer, when the trocar needle was piercing, cutting, and sliding through the foil at different defined loading phases and plotted as a load–displacement diagram. Magnified images of the consecutive cut were taken under a microscope after the entire penetration through the foil. Three physicians used all trocar systems in a masked fashion on human sclera to evaluate the manual penetration force in 30° and 90°.

**Results:** The mean outer diameter of the trocar systems was  $0.630 \pm 0.009$  mm, and the mean outer diameter of the trocars was  $0.750 \pm 0.013$  mm. The mean point length was  $3.11 \pm 0.49$  mm, and the mean length of the bevel was  $1.46 \pm 0.23$  mm. The primary bevel angle was  $10.75 \pm 0.41^\circ$ , and the secondary bevel angle was  $65.9 \pm 42.56^\circ$ . The piercing forces of the back bevel and spear-pointed trocars/needles were at the same level ( $0.087 \pm 0.028$  N). The lancet-pointed needle had remarkable low piercing and cutting forces with 0.41 N (range, 0.35–0.47 N). The spatula bevel tip showed the highest penetration piercing force with 1.6 N (range, 1.59–1.73 N). The back bevel systems induced frequently triangular-shaped incisions, with two nearly rectangular cuts of short length. The spear bevels produced a regular characteristic linear cut. Especially, the lancet blade created straight cut with a linear wound apposition. Spatula trocar systems caused usually an arched accurate incision. The manual force to penetrate the human sclera in an angled and rectangular angle appeared in the surgeons hand lower with a back bevel, lancet, or spear tip, whereas higher with spatula bevel systems.

**Conclusion:** Lancet and back bevel systems show less penetration force of inner needles than the spatula systems. The results of the penetration force experiments correlated well with the manual force on sclera.

RETINA 0:1–10, 2014

---

Microincision technology has changed the approach of vitreoretinal surgery since its introduction during the past decade.<sup>1–3</sup> Minimally invasive surgery in an outpatient setting offers patients convenience, the possibility of faster symptomatic recovery, and visual rehabilitation. The field has progressed from the initial 25-gauge systems, with their too flexible instruments and prolonged vitrectomy time, to current 23-gauge instrumen-

tation that overcomes most of these unwanted compromises, as well as modified stiffer 25-gauge systems with more efficient cutting, fluid dynamics, and improved illumination systems.<sup>2–8</sup> Thus modern microincision surgery has been quickly adopted by many surgeons in the worldwide retinal community.

Several recent advances in instrumentation for microincision surgery make this technology even better and

promising to increase the ease of surgery, reduce possible complications, and hopefully improve the functional and anatomical outcome for the patients. These enhancements include trocar blade designs to improve incision preparation, valved cannulas to prevent fluid leakage during surgery, and collagen plugs to aid closure of sclerotomy sites. Transconjunctival sutureless pars plana vitrectomy (PPV) has progressively been adopted as the first-choice technique for an increasing number of vitreoretinal surgeons because a number of significant advantages such as increased patient comfort with less postoperative inflammation, decreased operative times, and reduction of surgery-induced astigmatism become apparent.<sup>9–16</sup>

However, there is some disagreement about the best needle design for 23-gauge trocar systems. Recently, various modified user-friendly 23-gauge trocar systems have become available in the market. They vary in terms of the shape of the inner needle bevel, the bevel face size, the gap between the outer cannular and the inner needle, the shape of the outer catheter, the tapering method, and the material composition. All these features create a significant difference in the penetration force. Hence, we investigated the geometry, mechanical penetration force, and cutting profile of 11 currently commercially available types of 23-gauge trocar systems.

## Materials and Methods

### *Twenty-Three-Gauge Trocar Systems*

Eleven types of commercially available ophthalmologic trocar systems with a diameter for PPV were investigated in this experimental study (Table 1). All trocars and needles were carefully examined immediately after unpacking the blister package in their original state and removing the protecting plastic cap to detect, under a microscope, unexpected artificial damages before any penetration resistance measurement.

### *Nomenclature of the Needle Tip and Trocar*

The needles of trocar systems are generally composed of a protruded closed-ended stiletto with

a beveled face and taper tip, which are placed inside the orifice of the main needle tube. The outer cannula builds the trocar and has an outer 23-gauge diameter.

The bevel is the angled surface on a shaft of a sharpened stiletto to form a slanting edge at the needlepoint, facilitating an atraumatic penetration through the sclera into the human globe. The needlepoint, also known as “lancet point,” is the sharpest point available for any medical needles. The typical design of a needlepoint consists frequently of three bevel cuts: The primary bevel, which is the surfaced as a result of grinding the tube at a specific angle  $\alpha$ , and the two-side bevels, which are secondary grind angle  $\beta$  on each side of the primary bevel to form the cutting edge and a sharp needlepoint. The bevel length is by definition the longest distance of a bevel, measured from the tip of the needle to the most proximate area of grinding behind the heel. The side bevel length is measured between the juncture of side bevel, with the outside surface of the angled surface, and the tip of the needle.

The nomenclature for the front end of a stiletto can be divided by grinding and deburring in 4 main bevel type designs: “back” bevel (**A**), “spear” bevel (**B**), lancet bevel (**C**), and “spatula” bevel (**D**) (Figure 1):

- A. The back bevel design is characterized by an angled surface on the shaft of the stiletto to form a slanting edge at the sharpened needlepoint. The needle tip of the back bevel is sharply angled and has an edge behind the bevel. The stiletto has here a secondary grind on the opposing sides of the primary grinds. However, the bevel face of the back bevel needle is smaller compared with that of the lancet needles.
- B. The spear bevel design is characterized by an angled surface on the shaft of the stiletto to form a pyramid-like slanting triangular needlepoint. The needle tip of the spear bevel is sharply angled because of a secondary grind on the sides of the primary grinds.
- C. Lancet bevel point or diamond point has a needle tip with three bevels. A three-grind needlepoint formed from a primary grind and two secondary grinds. The broadest part of bevel diameter is bigger compared with the tip of back. However, it becomes tapered by 45° because of a second grind giving it the appearance of a diamond-shaped tip. The bevel face of the lancet needle is bigger than that of the back needle.
- D. Spatula bevel has no sharp needle tip in combination with a secondary bevel angle. The bevel is the beveled surface on a shaft to form a smooth closed-ended slanting junction with an oval tip to facilitate an atraumatic penetration, which appears sometimes more cumbersome to create a sclerotomy.

From the \*Department of Ophthalmology, University of Bonn, Bonn, Germany; †Eye Clinic Breyer, Dusseldorf, Germany; ‡Department of Ophthalmology, University of Sao Paulo, Sao Paulo, Brazil; and §Department of Ophthalmology, Southwest Hospital, Key Laboratory of Visual Damage and Repair of Chongqing Third Military Medical University, Chongqing, China.

C. H. Meyer and H. Kaymak contributed equally to the article. Paper presented in part at the 14th Annual EURETINA meeting 2014 London Bio-engineering Session: RETINATEC.

None of the authors have any financial/conflicting interests to disclose.

Reprint requests: Carsten H. Meyer, MD, Department of Ophthalmology, University of Bonn, Ernst-Abbe-Street 2, Bonn 53127, Germany; e-mail: meyer\_eye@yahoo.com

Table 1. Eleven Types of 23-Gauge Ophthalmologic Trocar Systems With Geometrical Data of the Trocar Bevel Needles Penetration Force Diagrams and Cut Images

Manufacture	Description	Size, Gauge	Bevel Type	Outside Diameter, mm	Point Length, mm	Bevel Length, mm	Primary Angle ( $\alpha$ ), in degrees	Secondary Angle ( $\beta$ ), in degrees	Outer Diameter Da (Cath)	Tip of Cath	Material of Cath
Geuder	Trocar system one step Hattenbach/Nicolic	23	Back	0.63	2.80 (2.78–2.91)	1.38 (1.35–1.41)	11.2 (11–11.5)	37 (35–38)	0.76	Blunt	Plast.
Geuder	Trocar system	23	Back	0.63	2.87 (2.75–3.0)	1.56 (1.53–1.63)	11.7 (11.5–12)	31 (30–32)	0.76	Blunt	Plast.
Alcon	Trocar blade 3CT	23	Back	0.63	2.89 (2.70–3.07)	0.97 (0.92–1.02)	10.8 (10.5–11)	72 (70–75)	0.74	—	—
Alcon	Entry system enhanced	23	Spear	0.62	2.55 (2.32–2.81)	1.56 (1.49–1.62)	10.8 (10–11)	—	0.74	Chamfer	Metal
Alcon	Entry system enhanced	23	Spear	0.62	2.38 (2.19–2.63)	1.55 (1.49–1.62)	10.7 (10.5–11)	—	0.74	Chamfer	Metal
Oertli	PMS autoseal one step	23	Back	0.65	3.05 (2.99–3.08)	1.49 (1.46–1.52)	10.4 (10–11)	31.8 (30–37)	0.78	Blunt	Metal
Oertli	PMS autoseal one step	23	Lancet	0.64	3.24 (3.11)	1.81 (1.82–1.83)	6	140	0.76	—	—
DORC	One step Cannula system	23	Spatula	0.63	3.96 (3.79–4.10)	—	Tip: 4; heel: 11	—	0.74	—	Metal
Fritz Ruck Eye Technology (Wefis)	Trocar set Disposable trocar set	23	Back	0.63	3.19 (2.98–3.31)	1.41 (1.35–1.52)	9.4 (9–10)	83.6 (80–89)	0.75	Chamfer	Metal
Bausch and Lomb	Loaded Clampshell PMP part: S-APX-B + L ESA	23	Spatula	0.64	3.49 (3.43–3.57)	—	9.5–10	—	0.73	Chamfer	Plast.
Min				0.62	2.3	0.97	10	31	0.73	2.27	
Max				0.65	3.96	1.81	11	140	0.78	4.49	
Mean		23		0.63	3.11	1.46	10.75	65.9	0.75	3.14	
Standard Deviation				0.009	0.49	0.23	0.41	42.56	0.013	0.5841	

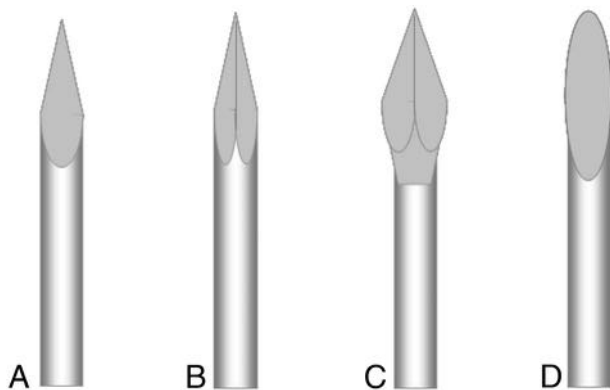


**Fig. 1.** Magnified schematic drawing of the front half of four examined trocar needle designs: back bevel (A), spear bevel (B), lancet bevel (C), and spatula bevel (D). An inner stiletto of trocar cannula systems was composed of a sharp tip with a beveled face on the main needle shaft. The left needle showed a bevel-faced needle. The next tip of the spear bevel was sharply angled in a triangular shape. The lancet bevel had the biggest diameter and an edge behind the primary bevel. The right tip of a spatula bevel had a round frontier by a backcut method.

### Normative Geometry

The tube dimensions are defined with the outer diameter and wall thickness. The individual geometrical data of the 11 different 23-gauge trocar systems were systematically analyzed according to the international nomenclature given in ISO 7864 (DIN 13097) and ISO 9626: The outside diameters of the trocar tube (da) and outside diameters of the solid catheter (da [cath]) were measured by Mitutoyo micrometer caliper (S/N 8225 258; Mitutoyo Corporation, Kawasaki, Japan). Point length and bevel length were measured with the Olympus stereo-microscope SZH (S/N 509 130; Olympus Corporation, Tokyo, Japan;  $\times 30$  magnification) on a cross table and x/y-micrometer. The primary bevel angle ( $\alpha$ ) and combined secondary back bevel angle ( $\beta$ ) were analyzed by a touchless laser optical inspection measuring station FACET (S/N me16). The details of the samples were listed in Table 1.

### Penetration Force Measurement

Penetration force measurement was performed according to DIN 13097. The tip of each trocar was positioned at a distance of 6 mm from the commonly used polyurethane foil (PU thickness, 0.040 mm; hardness shores,  $85 \pm 10$ ; free diameter, 10 mm) in a parallel direction (ISO 10555-5). The fixed standardized testing velocity of the push-pull motor on the needle was 100 mm per minute in  $90^\circ$  during all experimental measurements. The penetration resistance was precisely measured and plotted as a load-displacement diagram by Penetrometer DEKA 9 (DKA 0108; Melba, Leonberg, Germany), when the trocar/needle

was piercing the foil at different defined loading phases (Figure 2). The penetrometer had an established accuracy of  $\pm 5\%$  at a given test velocity of 100 mm per minute. All trocar samples and foils had to be stored at room temperature, 24 hours before testing. All the 23-gauge trocar systems were investigated and measured by 3 to 5 testing by individual probes under the same temperature condition.

The goal of a 23-gauge sclerotomy is to cut a “trap door” in the sclera that will close by intraocular pressure, as the trocar is withdrawn. When the needle tip contacted on the primarily intact membrane, the stiletto increased the pressure to the foil until it started to cut a hole in it (piercing force,  $F_0$ ). This primary load resulted in increased forces and deformation of material. After the initial cut, the foil material became displaced outwards along the bevel edges (cutting force,  $F_1$ ) until the complete diameter of the 23-gauge trocar passed through the hole in the foil (penetration force,  $F_2$ ). The measured bevel angles  $\alpha$  and  $\beta$  at the needle tip reflected the load of the displaced material. Smaller bevel angles frequently resulted in smaller transverse tip forces. As the complete diameter of the trocar passed progressively through the foil, friction along its edges became apparent (friction force,  $F_3$ ).

ISO measurements are important to compare in a standardized manner the penetration force of medical devices and needles. Although the experimental standards define the penetration speed and foil thickness, their results may be difficult to compare with surgical conditions during 23-gauge vitrectomy. In a second set of experiments, we offered 3 physicians, all 11 trocar systems in a blinded manner, and asked them to penetrate human sclera obtained from an eye bank. The penetration of the sclera was performed 3 times in a rectangular and  $30^\circ$  manner. The physicians were asked to judge their penetration force at the beginning (penetration) and complete insertion (sliding) through the sclera. The applied manual force was classified in five grades from one as blunt (high resistance) to five as very sharp (no resistance). The results of standardized experimental force measurements were compared with the manual findings.

### Magnified Images of the Consecutive Cut on the Penetrated Foil

Images were taken from each foil after the entire penetration process under a microscope (Olympus stereo-microscope SZH [S/N 509 130; Olympus Corporation];  $\times 20$  magnification). The resulting cut in the penetrated foil varied in length and form according to the applied bevel designs.

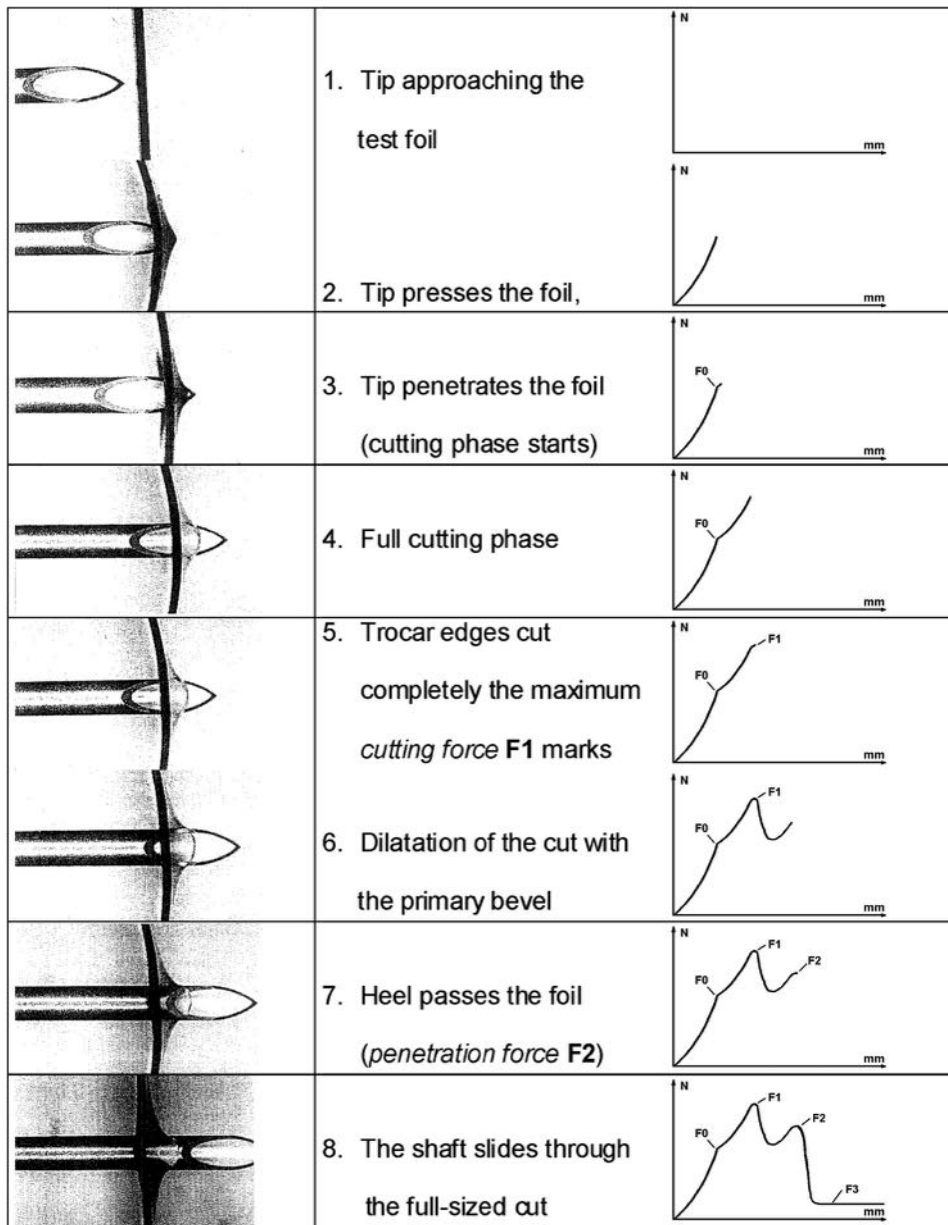


**Fig. 2.** Load-displacement diagram during penetration of the test foil with a trocar during different defined loading phases. The piercing force ( $F_0$ ) gradually increased as the needle tip penetrates the foil. The cutting force ( $F_1$ ) increased further until the edges cut to the complete diameter. Subsequently, the penetration force ( $F_2$ ) slightly decreased and erased afterward as the heel passed and dilated the foil. After the bevel slides passed through the foil, the friction force decreased rapidly ( $F_3$ ). The moments of the needle tip and resultant forces because of deformation of the medium during all phases of the dynamic rupture of soft solids are shown in the load-displacement diagram containing four characteristic phases: The first phase is characterized by the approaching of the needle tip and increasing resistance on the membrane. The punching property of a trocar during the penetration phase was increased. This phase ends with the penetration of the needle and a decline of force determined by a first peak  $F_0$  in the curve seen describing the tip resistance.  $F_0$  value is the maximum force to penetrate the foil. Blunt tip tend to lead to a steep increase. The second phase describes the entire penetration of the needle tip with its bevel up to the full diameter of the needle. Here, the sharpness of the bevel is measured as cutting resistance up to its maximum when the full diameter of the needle is inserted ( $F_1$  peak load).  $F_1$  is the maximum force from the cutting resistance. Blunt cutting edges lead to increases force. The third phase is the penetration of the needle, characterized by a dilatation of the cut until the heel passes completely with the full diameter measured as the third peak or

dilatation resistance  $F_2$ .  $F_2$  value is the maximum force from the dilatation resistance. The fourth phase characterizes the sliding of the shaft of the trocar and a decline of the friction resistance  $F_3$ .  $F_3$  value shows the friction force, which is hardly readable in these experiments.  $F_{cath}$  is the maximum force of the needle catheter/cannula. The fourth peak is the penetration resistance over the needle catheter tip (cannula tip).

## Results

### Geometry

All cut-bevel needles were evaluated by a single examiner who compared each needle for tip integrity or deformities. Variations from the manufacturer's standards included protrude stiletto beyond its needle tip, partial irregular tip separation in three samples led to the exclusion and replacement for the study. Geometrical data of all intact trocar needles are listed in Figure 3. Five trocar systems contained a back bevel design (Trocar system

one step, Trocar system; Geuder, Heidelberg, Germany), Trocar blade 3CT (Alcon, Fort Worth, TX), PMS Auto-seal one step (Oertli, Bern, Switzerland), Trocar set (Fritz Ruck, Eschweiler, Germany), two had a spear bevel (Entry system enhanced; Alcon). Only one trocar system used a lancet bevel (PMS Auto-seal one step; Oertli), whereas the other three preferred a spatula bevel design (One step Cannula system; DORC, Zuidland, the Netherlands), disposable trocar set (Eye technology, Rayleigh, United Kingdom), and Loaded Clampshell PMP (Bausch and Lomb GmbH, Berlin, Germany), respectively.

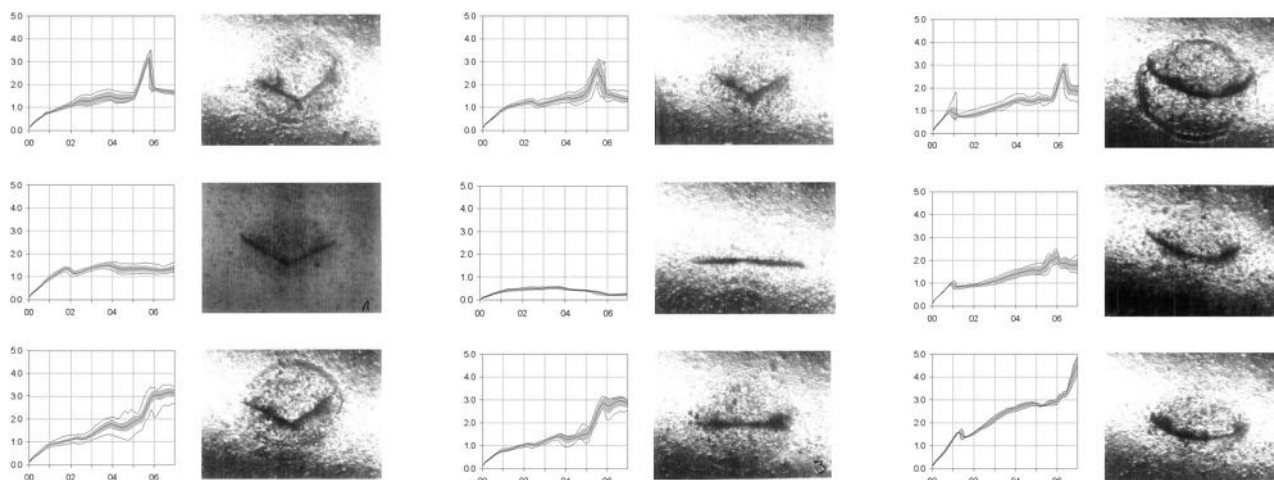


**Fig. 3.** Twenty-three-gauge trocar systems with penetration force diagrams and cut images. The left row shows three back bevel trocar systems from Geuder, Alcon, and Fritz Ruck. The middle row shows the back bevel from Oertli, the lancet bevel from Oertli, and spear bevel from Alcon. The right row shows three spatula bevels from Eyeteck, DORC, and Bausch and Lomb.

The mean outer diameter of the trocar system was  $0.630 \pm 0.009$  mm, and the mean outer diameter of trocar was  $0.750 \pm 0.013$  mm. The mean point length was  $3.11 \pm 0.49$  mm, and the mean length of the bevel was  $1.46 \pm 0.23$  mm. The primary angle ( $\alpha$ ) of the bevel was  $10.75 \pm 0.41^\circ$ , and the secondary back bevel angle ( $\beta$ ) was  $65.9 \pm 42.56^\circ$  (Figure 3). The measured parameters differed between varieties of spatula versions.

#### Penetration Force Measurement

The load–displacement diagram of a typical force graph of a medical needle penetrating a test foil and the magnified images of penetration pattern during different loading phases is shown in Figure 2. The measurements of the penetration force were listed in Table 1. The piercing forces ( $F_0$ ) of the back bevel and spear pointed trocars/needles were at the same level ( $0.87 \pm 0.28$  N). If the spatula tip was more similar to the single bevel tip forming a round cutting edge at tip instead of a pointed tip, it caused higher piercing forces than pointed tips. The lancet-pointed needle from Oertli had remarkable low piercing and cutting forces with 0.41 N (range, 0.35–0.47 N). The Bausch and Lomb trocar needle with the single spatula bevel tip showed a higher penetration piercing force with 1.6 N (range, 1.59–1.73 N).

The first 3 examples in Table 1 demonstrated back bevel trocar systems. The penetration force increased moderately when the back bevel needle tip became in contact with the foil and penetrated the foil. The penetration force increased significantly with the back bevel from Geuder and Oertli, as the needle heel passed through the foil and decreased also immediately afterward. The load–displacement diagram with

the back bevel from Alcon demonstrated no significant peak as the needle passes through the foil.

Examples 4 and 5 in Table 1 demonstrated the measurements with the spear bevel trocar systems from Alcon. The penetration force increased gradually when the needle tip contacted with the foil and penetrates the foil. The penetration force increased significantly with the spear bevel, as its needle heel passed through the foil. The slid-like cut seemed to maintain the shaft tight to the edge of the penetration hole, maintaining the force at higher levels.

Example 7 in Table 1 demonstrated the measurements with the lancet bevel trocar systems from Oertli. The penetration force increased minimally during all phases of the penetration. After the brought bevel end passed through and the catheter with a smaller diameter slid through the foil, there was no significant peak in the penetration forces ( $F_0$ ) measurement. The taper shape of the diamond bevel and longer slit-like cut may give space for gentle penetration of the shaft and a low penetration force; 0.41 N (range, 0.35–0.47 N) was the lowest penetration force among all experiments.

Examples 8, 10, and 11 in Table 1 demonstrated the measurements with the spatula bevel trocar systems from DORC, Eye technology, and Bausch and Lomb. The mean penetration force ( $F_0$ ) was above the average. It was increased significantly when the needle tip came in contact with the foil and penetrated the foil. The flat angle of the tip and its characteristic increased, and curved shaped of the cut might be responsible for this profile. Subsequently, a sudden increase in force was observed, when the catheter tip reached the foil and then rapidly decreased after point passed through the foil.

### *Manual Scleral Penetration*

All 11 trocar systems were used in a randomized blinded order and penetrated the human sclera 3 times in a rectangular and 30° manner. The applied manual force at the beginning (piercing) and complete insertion (sliding) through the sclera was classified in five grades from one as blunt (high resistance) to five as very sharp (no resistance): The applied manual force with the back bevel and spear tip was graded between 3.0 and 4.0 as “moderate sharp.” The applied manual force with the lancet bevel was noticed as “sharp” with grades between 4.0 and 4.5. The applied manual force with the spatula bevel was “more cumbersome” and was graded from 2.0 to 3.5. There was no main difference in the evaluation between the three surgeons. It was difficult for the surgeons to differentiate between the early piercing and late sliding of the penetration experiment because the duration of the entire process was short. Minor subjective changes are documented in Table 2. The graded manual piercing force in a 30° (Table 2) and rectangular fashion did also not differ for the surgeons. There was a good correlation between the standardized experimental measurements and the clinical surgical manual penetration of the trocar in the surgeons hand under surgical conditions.

### *Magnified Images of the Consecutive Cut on the Penetrated Foil*

The magnified images show for each individual trocar system the performed penetration cut on the corresponding penetrated area (Table 2). The uniform exercised penetration experiments highlighted a correlation of the individual “trocar tip” and the cutting pattern on the foil. Some individual cuts showed an additional circle around the cut, which reflect the indentation of the trocar tip on the foil. The magnified images demonstrate a clear correlation of the applied trocar design with the repeatedly achieved cut pattern: The back bevel trocar systems induced frequently triangular-shaped incisions, with two nearly rectangular cuts of short length and good wound architecture. The spear and lancet bevels produced a regular characteristic linear cut. Especially, the lancet blade created a straight cut with a linear wound apposition. Spatula trocar systems caused usually an arched accurate, sometimes, chevron-shaped cut. Some vaulted inclined incisions appeared asymmetrical with less stable wound architecture, possibly leading to incomplete closure and leakage.

## **Discussion**

Current transconjunctival 23- and 25-gauge trocar systems provide a self-sealing option, as the surgical

wound seals and heals without sutures because of its smaller incision size.<sup>17–20</sup> Most 23-gauge trocar inserters currently contain a sharp needle-like entry stiletto device that creates a linear or curved cut through the scleral wall.<sup>21–24</sup> The outer segment of the trocar is generally cylindrical, as the surgeon pivots the surgical instrument into the globe. The 23-gauge trocar system is usually self-sealing, limited to inflammation, which may shorten the consecutive visual recovery, as compared with previous sutured 25-gauge procedures.<sup>11,25–27</sup>

Various parameters play a role during the initial piercing process, including the tip of the trocar (sharpness), the thickness and individual rigidity of the scleral resistance, and intraocular pressure of the patient’s eye. The pressure, necessary for puncture, is predominantly influenced by the composition of the tissue, whereas the total force, needed to reach this pressure, is governed by the area of the trocar point (pressure = force per unit area). The initial puncture, which begins with the insertion procedure, is accomplished when the distal end of the trocar needle tip applies enough pressure (F1) to cause the tissue structure to displace (F2). The length and form of the performed cut may influence the dilatation force (F3) and friction force (F4).<sup>28</sup> These findings have been evaluated in clinical settings. Although small-gauge needles and beveled incision techniques are commonly also recommended for intravitreal injections, we evaluated in 205 eyes the amount of reflux and degree of pain with intravitreal injection using 26-, 27-, 29-, and 30-gauge needles.<sup>25</sup> Patients injected with the larger 26- or 27-gauge needle experienced more pain and greater reflux compared with injections performed with a 29- or 30-gauge needle. However, the degree of reflux was only significant, when the no beveled incision technique was used. The beveled scleral incision showed benefit in performing intravitreal injections. Small incisions and a proper closure of the scleral wound are important to prevent leakage after intravitreal injections and small gauge PPVs.

The most important factor in reducing penetration forces is related to the unique design of the edges on the bevel face. Here, we analyzed the geometrical data of different 23-gauge trocar systems and identified four different bevel types of the trocar needles (back bevel, spear bevel, lancet bevel, and spatula bevel). Our experimental study allowed us to compare the applied penetration forces and achieve penetrating cuts of various 23-gauge trocars commercially available for PPV. To assess the impact of the shape of the trocar systems in an equal manner, our measurements were performed under standardized ISO laboratory conditions.

We demonstrated that the performance of the stiletto insertion follows four characteristic phases. The

Table 2. Measured Forces of the Different Trocar Systems During the Experimental and Manual Penetration Experiments

Manufacturer	Description	Size	F0 Mean (Min–Max [N])	F1 Mean (Min–Max [N])	F2 Mean (Min–Max [N])	F3 Mean (Min–Max [N])	F <sub>Cath</sub> Mean (Min–Max [N])	Manual Force Piercing	Manual Force Sliding
Geuder	Trocar system one step Hattenbach/ Nicolic	23 G	0.78 (0.72–0.86)	1.10 (0.95–1.1)	1.0 (0.69–1.10)	0.85	3.05 (2.63–3.34)	3.7 (3.5–4.0)	3.8 (3.5–4.0)
Geuder	Trocar system	23	0.80 (0.71–0.83)	1.27 (1.10–1.54)	1.48 (1.30–1.79)	1.39	3.27 (3.09–3.51)	3.7 (3.5–4.0)	4.0 (3.5–4.0)
Alcon	Trocar blade 3CT	23	0.89 (0.78–0.93)	1.34 (1.22–1.43)	1.49 (1.33–1.64)	1.34 (1.15–1.57)	–	3.5 (3.0–4.0)	4.1 (3.0–4.0)
Alcon	Entry system enhanced	23	0.76 (0.72–0.81)	1.0 (0.94–1.1)	1.40 (1.20–1.51)	1.39	3.02 (2.62–3.17)	3.8 (3.5–4.0)	4.0 (3.5–4.0)
Alcon	Entry system enhanced	23	0.79 (0.71–0.87)	1.15 (0.95–1.29)	1.77 (1.31–2.09)	1.65	3.27 (2.92–3.50)	3.8 (3.0–4.0)	4.0 (3.0–4.0)
Oertli	PMS autoseal one step	23	0.85 (0.80–0.89)	1.24 (1.13–1.38)	1.40 (1.20–1.67)	1.38	2.97 (2.63–3.14)	3.7 (3.0–4.0)	3.7 (3.0–4.0)
Oertli	PMS autoseal one step	23	0.41 (0.35–0.47)	0.48 (0.41–0.56)	0.52 (0.47–0.58)	0.21 (0.20–0.22)	–	4.2 (4.0–4.5)	4.0 (4.0–4.5)
DORC	One step Cannula system	23	1.0 (0.9–1.07)	–	1.58 (1.37–1.84)	1.55	2.27 (1.99–2.50)	3.0 (2.5–3.5)	3.0 (2.5–3.5)
Fritz Ruck Eye Technology (Wefis)	Trocar set Disposable trocar set	23	0.76 (0.75–0.76)	2.16 (1.77–2.37)	2.36 (2.17–2.63)	2.30	3.09 (2.97–3.27)	4.0 (3.5–4.5)	4.0 (3.5–4.5)
Bausch and Lomb	Loaded Clampshell PMP part: S- APX-B + L ESA	23	1.6 (1.59–1.73)	–	2.83 (2.72–2.88)	2.74	4.49 (4.07–4.83)	2.5 (2.0–3.0)	3.5 (2.0–3.5)
Min			0.41	0.48	0.52	0.21	2.27	2.5	3.0
Max			1.6	2.16	2.83	2.74	4.49	4.2	4.1
Mean		23	0.87	1.21	1.57	1.47	3.14	3.8	4.0
Standard Deviation			0.28	0.46	0.61	0.65	0.58	0.5	0.7

penetration resistance of the bevel tip was for the major number of tested types at about the same level even for the blunt versions. Lancet blades had remarkable low piercing and cutting forces, inducing a symmetrical wound architecture and linear wound apposition (Table 2). The piercing force of the “back” and spear bevel pointed trocars/needles were at the average level. DORC trocar needle had a very flat long spatula with a slim tip but only slightly lower penetration resistance. The Bausch and Lomb trocar needle also showed a higher resistance with 4.5 N. Here, it seems to be harder to ensure a proper closure with a chevron-shaped incision than with a linear incision. Our study showed that spear and lancet bevels produced a linear incision, whereas the back bevel caused triangular-shaped format. Although spatular trocar systems induce an accurate incision and appeared less stable, possibly leading to inclined cuts or even sometimes chevron-shaped cuts with less stable wound architecture, and an incomplete closure, possibly leading to postoperative leakage.

All trocar systems were used to penetrate sclera in a rectangular and 30° manner. The applied manual force was graded as moderate sharp with the back bevel and spear tip, as sharp with the lancet bevel tip, and more cumbersome with the spatula bevel tip. It was difficult for the surgeons to differentiate between the early piercing and late sliding of the penetration experiment because of the short duration of the entire process. The applied angle did not affect the force. This observation correlated well with previous experiments where we demonstrated that the angle of the injection did also not affect the pain level for the patient.<sup>25</sup> In addition, we applied recently the same penetration force experiment to the Ozurdex drug application system with the old and new needle design and measured significant lower penetration force with the new needle design.<sup>29</sup> A comparison between the here investigated 23-gauge pars plana trocar systems and 22-gauge DDS-applicator systems demonstrated lower penetration forces (F0) (0.7 N for the old and 0.47 N for the new DDS-applicator needles), whereas 23-gauge trocar systems like the spatula bevel tip required significant higher penetration forces (1.6 N; range, 1.59–1.73 N) to penetrate the same foil under standardized condition according to ISO 10555-5. However demonstrated similar measurements of conventional medical needles lower forces to penetrate the standardized 0.4-mm foil, the measured values were 0.54 N for F0, 0.58 for F1, 0.76 N for F2 for a 29-gauge Klinion needle and 0.42 N for F0, 0.43 N for F1, 0.63 N for F2 for a 31-gauge Klinion needle. All the experimental studies demonstrated that the needle design and sharpness affect the manual force in the surgeons hand to penetrate the sclera of the patient.

Most vitreoretinal surgeons realize and prefer today improved novel surgical bevel geometry for 23-gauge transconjunctival vitreoretinal surgery.<sup>30–32</sup> Using these novel blades, the surgeon creates a self-sealing surgical wound, first by directing the surgical blade substantially parallel to the eye surface, then redirecting the blade to follow the general curvature of the eye globe, and finally redirecting the blade to enter the interior of the eye. The enhanced surgical blades have two main advantages: 1) a rigid wide-mouthed outer segment and 2) a generally thin-walled collapsible plastic polymer or metal mesh sleeve that spans the surgical wound and substantially adapts to its natural geometrical contour.

In summary, instrumentation for microincision vitreoretinal surgery has evolved to enable delicate maneuvers in a closed space under a microscope. More recent beveled trocar blades represent a significant improvement over earlier needle-style trocars, reducing the amount of required mechanical force to penetrate tissue and insert the trocar system. We investigated trocar systems and demonstrated improvement in design modifications, manufacturing techniques, and sharpness. Current innovations accomplished less resistance of the blade to the tissue, achieved a smooth trocar insertion, and facilitated more efficient wound closure with better healing characteristics. Although some spatula systems still require high penetration, others had remarkable low piercing and cutting forces. To improve on these findings, we are still striving to find the perfect trocar needle design for 23-gauge PPV.

## Conclusion

Newer beveled trocar blades represent a significant improvement, reducing the amount of required force to penetrate tissue and insert the cannula system. The accomplished cut profile demonstrated good wound architecture in most of the cases. These findings, in a standardized ISO laboratory, will support ongoing innovations to improve 23-gauge trocar systems of PPV.

**Key words:** sclerotomy, 23-gauge, trocar system, pars plana vitrectomy, penetration force, grinding method, bevel.

## References

1. Fujii GY, de Juan E, Humayun MS, et al. A new 25-gauge instrument system for transconjunctival sutureless vitrectomy surgery. *Ophthalmology* 2002;109:1807–1812.
2. Eckardt K. Transconjunctival sutureless 23-gauge vitrectomy. *Retina* 2005;25:208–211.
3. Thompson JT. Advantages and limitations of small gauge vitrectomy. *Surv Ophthalmol* 2011;56:162–172.
4. Charles S. Vitreoretinal instrumentation, surgical fluidics. In: Saxena S, Meyer CH, Ohji M, Akduman L, eds. *Vitreoretinal*

- Surgery. New Delhi, India: Jaypee Medical Publishers; 2012: 15–33.
5. Lopez-Guajardo L, Pareja-Esteban J, Teus-Guezala MA. Oblique sclerotomy technique for prevention of incompetent wound closure in transconjunctival 25-gauge vitrectomy. *Am J Ophthalmol* 2006;141:1154–1156.
  6. Hsu J, Chen E, Gupta O, et al. Hypotony after 25-gauge vitrectomy using oblique versus direct cannula insertions in fluid-filled eyes. *Retina* 2008;28:937–940.
  7. Singh RP, Bando H, Brasil OF, et al. Evaluation of wound closure using different incision techniques with 23-gauge and 25-gauge microincision vitrectomy systems. *Retina* 2008;28:242–248.
  8. Inoue M, Noda K, Ishida S, et al. Intraoperative breakage of a 25-gauge vitreous cutter. *Am J Ophthalmol* 2004;138:867–869.
  9. Shinoda H, Nakajima T, Shinoda K, et al. Jamming of 25-gauge instruments in the cannula during vitrectomy for vitreous haemorrhage. *Acta Ophthalmol* 2008;86:160–164.
  10. Inoue M, Shinoda K, Shinoda H, et al. 25-gauge cannula system with microvitreoretinal blade trocar. *Am J Ophthalmol* 2007;144:302–304.
  11. Inoue M, Shinoda K, Hirakata A. Twenty-three gauge cannula system with microvitreoretinal blade trocar. *Br J Ophthalmol* 2010;94:498–502.
  12. Faia LJ, McCannel CA, Pulido JS, et al. Outcomes following 25-gauge vitrectomies. *Eye (Lond)* 2008;22:1024–1028.
  13. Parolini B, Prigione G, Romanelli F, et al. Postoperative complications and intraocular pressure in 943 consecutive cases of 23-gauge transconjunctival pars plana vitrectomy with 1-year follow-up. *Retina* 2010;30:107–111.
  14. Scott IU, Flynn HW Jr, Acar N, et al. Incidence of endophthalmitis after 20-gauge vs 23-gauge vs 25-gauge pars plana vitrectomy. *Graefes Arch Clin Exp Ophthalmol* 2011;249:377–380.
  15. Meyer CH, Rodrigues EB, Schmidt JC, et al. Sutureless vitrectomy surgery. *Ophthalmology* 2003;110:2427–2428.
  16. Taban M, Ventura AA, Sharma S, Kaiser PK. Dynamic evaluation of sutureless vitrectomy wounds: an optical coherence tomography and histopathology study. *Ophthalmology* 2008;115:2221–2228.
  17. Fabian ID, Moisselev J. Sutureless vitrectomy: evolution and current practices. *Br J Ophthalmol* 2011;95:318–324.
  18. Hubschman JP, Bourges JL, Tsui I, et al. Effect of cutting phases on flow rate in 20-, 23-, and 25-gauge vitreous cutters. *Retina* 2009;29:1289–1293.
  19. Machado LM, Magalhães O Jr, Maia M, et al. Comparison of 20-, 23-, and 25-gauge air infusion forces. *Retina* 2011;31:2002–2006.
  20. Gupta OP, Maguire JJ, Eagle RC Jr, et al. The competency of pars plana vitrectomy incisions: a comparative histologic and spectrophotometric analysis. *Am J Ophthalmol* 2009;147:243–250.
  21. Lopez-Guajardo L, Benitez-Herreros J, Silva-Mato A. Experimental model to evaluate mechanical closure resistance of sutureless vitrectomy sclerotomies using pig eyes. *Invest Ophthalmol Vis Sci* 2011;52:4080–4084.
  22. Leitritz MA, Spitzer MS, Bartz-Schmidt KU. New forceps for 1-step valve-free 23-gauge vitrectomy. *Retina* 2011;31:810–811.
  23. Oshima Y, Wakabayashi T, Sato T, et al. 27-gauge instrument system for transconjunctival sutureless microincision vitrectomy surgery. *Ophthalmology* 2010;117:93–102.
  24. Inoue M, Ota I, Taniuchi S, et al. Miyake-Apple view of inner side of sclerotomy during microincision vitrectomy surgery. *Acta Ophthalmol* 2011;89:e412–e416.
  25. Rodrigues EB, Grumann A Jr, Penha FM, et al. Effect of needle type and injection technique on pain level and vitreal reflux in intravitreal injection. *J Ocul Pharmacol Ther* 2011;27:197–203.
  26. Yamane S, Takemae K, Inoue M, et al. Evaluation of microincision vitrectomy wounds made with microvitreoretinal blade or beveled trocar by swept source optical coherence tomography. *Retina* 2012;32:140–145.
  27. Wu PC, Tiong IS, Chuang YC, Kuo HK. Twisting maneuver for sutureless vitrectomy trocar insertion to reduce intraoperative intraocular pressure rise. *Retina* 2011;31:887–892.
  28. Sitzman BT, Uncles DR. The effects of needle type, gauge, and tip bend on spinal needle deflection. *Anesth Analg* 1996;82:297–301.
  29. Meyer CH, Liu Z, Rodrigues EB, Brinkmann CK. Penetration force, geometry and cutting profile of the novel and old Ozurdex needle: the MONO-study. *J Ocul Pharmacol Ther* 2014.
  30. Ehrlich R, Goh YW, Ahmad N, Polkinghorne P. Retinal breaks in small-gauge pars plana vitrectomy. *Am J Ophthalmol* 2012;153:868–872.
  31. Wu WC, Lai CC, Lin RI, et al. Modified 23-gauge vitrectomy system for stage 4 retinopathy of prematurity. *Arch Ophthalmol* 2011;129:1326–1331.
  32. Horozoglu F, Yanyali A, Macin A, et al. 23-gauge transconjunctival sutureless vitrectomy for retained lens fragments after complicated cataract surgery. *Retina* 2012;32:493–498.